JBC RESEARCH ARTICLE

Streamlining assays of glycosyltransferases activity using *in vitro* GT-array (*i*-GT-ray) platform: Application to family GT37 fucosyltransferases

Received for publication, December 12, 2023, and in revised form, January 30, 2024 Published, Papers in Press, February 7, 2024,
https://doi.org/10.1016/j.jbc.2024.105734

Matrika Bhattarai[1], Qi Wang[2], Tasleem Javaid[1], Akshayaa Venkataraghavan[1], Md Tanim Al Hassan[2], Malcolm O'Neill[3], Li Tan[3], Hao Chen[2], and Ahmed Faik[1,*]

From the [1]Department of Environmental and Plant Biology, Ohio University, Athens, Ohio, USA; [2]Department of Chemistry & Environmental Science, New Jersey Institute of Technology, Newark, New Jersey, USA; [3]Complex Carbohydrate Research Center, University of Georgia, Athens, Georgia, USA

Reviewed by members of the JBC Editorial Board. Edited by Chris Whitfield

Numerous putative glycosyltransferases (GTs) have been identified using bioinformatic approaches. However, demonstrating the activity of these GTs remains a challenge. Here, we describe the development of a rapid *in vitro* GT-array screening platform for activity of GTs. GT-arrays are generated by cell-free *in vitro* protein synthesis and binding using microplates precoated with a N-terminal Halo- or a C-terminal GST-tagged GT-encoding plasmid DNA and a capture antibody. These arrays are then used for screening of transferase activities and the reactions are monitored by a luminescence GLO assay. The products formed by these reactions can be analyzed directly from the microplates by mass spectrometry. Using this platform, a total of 280 assays were performed to screen 22 putative fucosyltransferases (FUTs) from family GT37 (seven from Arabidopsis and 15 from rice) for activity toward five acceptors: non-fucosylated tamarind xyloglucan (TXyG), arabinotriose (Ara_3), non-fucosylated rhamnogalacturonan I (RG-I), and RG-II from the *mur1-1* Arabidopsis mutant, and the celery RG-II monomer lacking Ara*p* and MeFuc of chain B and L-Gal of chain A. Our screen showed that *At*FUT2, *At*FUT5, and *At*FUT10 have activity toward RG-I, while *At*FUT8 was active on RG-II. Five rice *Os*FUTs have XyG-FUT activity and four rice *Os*FUTs have activity toward Ara_3. None of the putative *Os*FUTs were active on the RG-I and RG-II. However, promiscuity toward acceptors was observed for several FUTs. These findings extend our knowledge of cell wall polysaccharide fucosylation in plants. We believe that *in vitro* GT-array platform provides a valuable tool for cell wall biochemistry and other research fields.

All cells have an extracellular matrix constructed from various types of carbohydrates and glyco-conjugates. These glycans are assembled by enzymes referred to as glycosyltransferases (GTs) (1). A large number of putative GTs have been identified using bioinformatic approaches. The carbohydrate-active enzymes database (CAZy, www.cazy.org) currently classifies GTs into 117 families (as of November 2023) and also contains many GTs assigned to no family at all. However, only a few members in each family have had their biochemical function(s) confirmed experimentally. For example, the GT2 family, which includes synthases involved in the synthesis of cellulose, chitin, mannan, mixed-linkage-glucan, and glycosylated secondary metabolites, contains 10,731 proteins from eukaryotes, of which, less than 2% have been functionally characterized. This is due in large part to several technical difficulties. Most eukaryotic GTs are integral membrane proteins and are difficult to purify (2, 3). The amounts of GT proteins and their corresponding mRNAs are low in cells. Predicting the donor/acceptor specificities of GTs from their sequences alone is not reliable. In addition, high-throughput tools for screening of GT activities are lacking.

The extracellular matrix of plants is referred to as the cell wall. This wall is considered to be a dynamic structure and have an essential role in plant growth and development, as well as in a plants ability to adapt to changing environmental conditions (4, 5). Cellulose, hemicellulose, and pectin account for the bulk of the polysaccharides present in the primary wall that surrounds growing plant cells. The main monosaccharides used to form these polysaccharides are glucose (Glc), galactose (Gal), arabinose (Ara), galacturonic acid (GalA), xylose (Xyl), and rhamnose (Rha). Lower amounts of fucose (Fuc, 6-deoxy-L-Gal), methyl fucose, apiose (a branched-chain pentose with a tertiary alcohol), methyl Xyl, aceric acid (a branched acidic hexose), glucuronic acid (GlcA), 3-keto-D-manno-octulosonic acid (Kdo), and 3-keto-D-lyxo-heptulosaric acid (Dha) are also present (6). Fucosylated cell wall polysaccharides are believed to have a role in many physiological processes. For example, virtually no Fuc is present in the walls of the Arabidopsis *mur1* mutant, which has lost the ability to produce GDP-L-Fuc, the activated sugar donor used by fucosyltransferases (FUTs). These walls have reduced mechanical strength, which leads to reduced growth (7–9). Cell wall fucosylation may be associated with tolerance to freezing temperatures (10), influences control of leaf water loss, and alters stomatal development and mechanical properties (11). Fucosylation may also have a role

* For correspondence: Ahmed Faik, faik@ohio.edu.
Present address for Tasleem Javaid: Complex Carbohydrate Research Center, 315 Riverbend Rd. University of Georgia, Athens, GA 30602.

in the formation of lignified tissue through activation of jasmonic acid signaling pathway (12). Many of these effects have been attributed to reduced fucosylation of cell wall pectins and the inability of the plants to form normal amounts of the borate crosslinked rhamnogalacturonan (RG) dimer (9).

It has been estimated that at least 67 different GTs including several FUTs are required for pectin biosynthesis (13). These FUTs add Fuc residues to RG-I and RG-II. Fuc is α(1,2)-linked to Gal in type-I and type-II arabinogalactan (AG) side chains (14). In RG-II, MeFuc is α(1,2)-linked to Gal in side chain B, whereas the Fuc in side chain A is α(1,4)-linked to Rha (13, 15). No FUTs specific for RG-I and RG-II have been identified. The CAZy database classifies FUTs into 7 GT families according to the type of linkage formed by these enzymes (16). Families GT37 and GT11 contain mostly α(1,2) FUTs. Family GT10 contains α(1,3)/(1,4) FUTs. Family GT23 contains α(1,6) FUTs. Protein *O*–fucosyltransferases (POFUTs) have been assigned to families GT41, GT65, and GT68. Only FUTs from families GT10, GT37, GT41, and GT65 are present in plants. The only plant cell wall polysaccharide FUTs with known functions are from family GT37. Arabidopsis *At*FUT4 and *At*FUT6 catalyze fucosylation of AG proteins (AGPs) (17), whereas Arabidopsis *At*FUT1 (18), pea (*Ps*FUT) (19), and rice *Os*MUR2 (Os02g0764200) (20) catalyze fucosylation of XyG. It has been suggested that all the putative FUTs of family GT37 catalyze the formation of a α(1,2)-linkage in plant cell wall polysaccharides. Advances in bioinformatic based on evolutionary relationships (phylogeny) (21–24) have assisted functional predictions for many GTs. However, this approach failed in predicting the function or substrate specificity of the FUTs in family GT37 because they cluster in clades by species rather than by similarity of enzyme activity (20, 25–27). Thus, the function of a FUT from GT37 family must be determined by defining enzyme activity *in vitro* or by mutant complementation.

In this work, we developed a platform *in vitro* GT-array (*i*-GT-ray) that simplifies the screening of transferase activity *in vitro*. The *i*-GT-ray platform is based on a recently developed method called nucleic acid programmable protein array (NAPPA), which has been widely used in protein-protein interactions (PPIs) studies in animals (28–31), Arabidopsis (32), and more recently, was applied to demonstrate PPIs between GTs on microplates (33). In the original NAPPA method, glass slides are coated with N-terminal Halo- or C-terminal GST-tagged GT plasmid DNA and an anti-tag capture antibody (CAb), which allows protein production using cell-free *in vitro* protein synthesis and protein capture on glass slide. Since GTs produced on microplates can engage in PPIs, strongly suggests that these GTs have proper folding *in vitro* and should maintain their transferase activity. Thus, we sought to adapt this method for GT assays on microplates and named it *i*-GT-ray platform. GT arrays were generated by precoating microplates with plasmid DNA and CAb (anti-tag antibody), which can be used for the production of tagged GTs (*via* cell-free *in vitro* protein synthesis) and capture on the microplate (Fig. 1). The *i*-GT-ray screening platform is more efficient and rapid than heterologous expression and purification of proteins for screening GT activities. The possible use of desalting paper spray-mass spectrometry (DPS-MS) detection method (in addition to GLO system) was demonstrated through detection of the products formed by transferase reactions of three GTs (AtXXT1, AtGUX1, and AtFUT6) directly from the microplates (34) (Fig. 1).

Using *i*-GT-ray platform, we performed a total of 280 assays (including the controls and duplicates) to screen 22 putative FUTs (seven from Arabidopsis and 15 from rice) from family GT37 for activity toward five acceptors: non-fucosylated tamarind XyG (TXyG), arabinotriose (Ara_3), non-fucosylated RG-I(*mur1*) and RG-II(*mur1*) prepared from the Arabidopsis *mur1-1* mutant, and RG-II (-L-Gal,-MeFuc), obtained by removing Ara*p* and MeFuc from chain B and L-Gal from chain A of the de-esterified celery RG-II monomer. Our screen showed that *At*FUT2, *At*FUT5, and *At*FUT10 have activity toward RG-I, while *At*FUT8 is active on RG-II. Five rice *Os*FUTs have XyG-FUT activity and four rice *Os*FUTs have activity toward Ara_3. None of the putative *Os*FUTs were active on the RG-I and RG-II acceptors used in this study. Screening of enzyme activities of some putative rice *Os*FUTs using GLO system is a starting point for detailed studies to improve and expand our understanding of plant cell wall fucosylation mechanisms, which should allow comparisons between rice and Arabidopsis and help elucidate how FUTs from GT37 family function.

Results

Implementing the i*-GT-ray platform for high-throughput* in vitro *screening of nonprocessive GTs*

Our goal was to develop a pipeline for high-throughput screening of GT activities by combining *in vitro* transcription/translation (IVTT)-based protein synthesis and enzyme assays on microplates with product detection (Fig. 1). To achieve this goal, optimization at several levels were performed. Since most eukaryotic GTs are membrane proteins and often difficult to produce *in vitro* as soluble, full-length active forms (2, 3), we reasoned that adding a GST or haloalkane dehalogenase (Halo) tag would improve solubility without impacting enzyme activity. This approach was validated previously with the nonprocessive Arabidopsis GTs *At*XXT1 and *At*GUX1 (34). Here, we used three additional nonprocessive GTs (*At*FUT1, *At*FUT6, and *At*MUR3) to optimize our *i*-GT-ray platform (Table S1 lists all GTs used in the optimizations). We first compared the efficiency of two cell-free coupled IVTT expression systems (TNT Quick System and 1-Step Human Coupled IVT Kit.) in producing the tagged GTs. Western blotting analysis was performed to confirm the presence and estimate the amounts of fusion proteins produced by each system. Our results indicated that the 1-Step Human Coupled IVT system produced similar amounts of fusion proteins (∼25 ng/μl) for each GT without substantial degradation (Fig. S1). The GTs produced by the TNT Quick expression system were degraded and Western blot analysis showed high background (Fig. S1). Thus, the 1-Step Human Coupled IVT system was used in all further experiments.

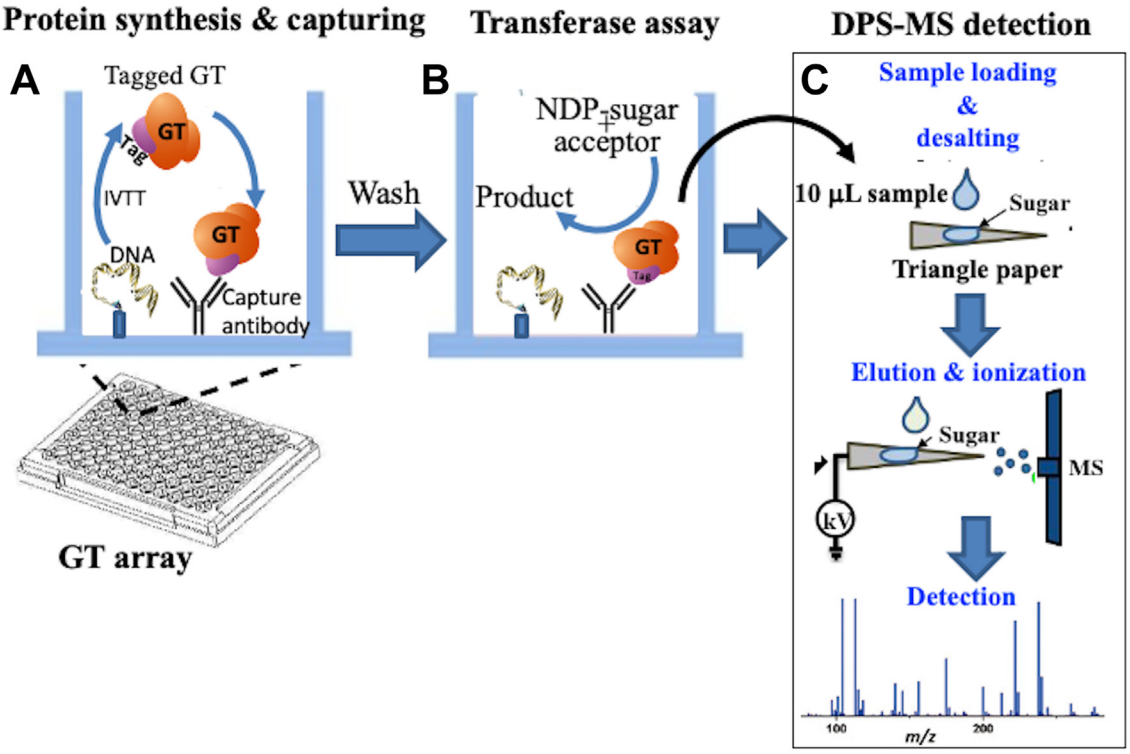

Figure 1. Schematic presentation of the *i*-GT-ray screening platform coupled with DPS-MS detection method. *A*, capture antibody and biotinylated plasmid DNA are immobilized on microplates, which is used to couple protein synthesis (*via* IVTT system) and capturing on microplate to create a GT-array. *B*, GT-array is then used for transferase assay using NDP-sugar donors and acceptors. *C*, products generated by transferase reactions can be detected through DPS-MS. DPS-MS, desalting paper spray-mass spectrometry; GT, glycosyltransferase; *i*-GT-ray, *in vitro* GT-array; IVTT, *in vitro* transcription/translation; NDP, nucleotide diphosphate.

The next step was to determine the optimal dilutions of the CAb (anti-GST or anti-Halo) needed in microwells to capture the fusion proteins in amounts sufficient for detection of transferase activity. Thus, we precoated microplates with three different dilutions (1/50, 1/200, and 1/400) of the CAb. The tagged GTs were then added to the microwells. *At*FUT1, *At*XXT1, and *At*GUX1 (as N-terminal Halo- or C-terminal GST-tagged) were used, and their transferase activities analyzed according to published protocols (see Table S1 for references) using the GLO system, which is a sensitive bioluminescent assay for the detection of UDP or GDP released from nucleotide diphosphate (NDP)-sugars by a transfer reaction. The acceptors used for *At*FUT1, *At*XXT1, and *At*GUX1 were TXyG, cellohexaose (C_6), and xylohexaose (X_6), respectively. Our findings show that the anti-GST and anti-Halo GTs gave higher activity in microwells precoated with CAb diluted to 1/50 and 1/200 (Fig. 2*A*). The position of the tag in fusion proteins had no discernible effect on the activity of *At*XXT1 and *At*GUX1 attached to microwells. By contrast, the C-terminal GST-tagged version of *At*FUT1 showed no transferase activity (Fig. 2*A*). This result was consistent with data obtained using an assay performed with radiolabeled donor substrate (Fig. S2).

High-throughput screening requires the use of comparable assay conditions (buffer and ions) for each GT. Thus, we next determined whether specific buffer/ion conditions can be used for most GTs. For this experiment, we tested the activity of N-terminal Halo-tagged *At*FUT1, *At*GUX1, and *At*MUR3 in 50 mM Hepes or Tris–HCl, pH 7, containing Mg^{++} and Mn^{++} (1 mM each). For *At*MUR3, partially degalactosylated nasturtium XyG was used as the acceptor (35). Hepes buffer is widely used in GT assays, but causes ion suppression in mass spectrometry (MS). Tris–HCl buffer is compatible with MS detection (34, 36), but not commonly used for GT assays. All three GTs were active in both buffers (Fig. S3). Although the activity levels were somewhat lower in Tris–HCl compared to Hepes, we concluded they were sufficient for high-throughput screening.

Next, we optimized the immobilization of both plasmid DNA and CAb (at 1/200) to allow simultaneous protein synthesis and capturing on the microwells (Fig. 1). DNA immobilization was carried out using a "streptavidin-biotin" system (37). We choose this system because streptavidin has four subunits into which four biotin molecules are strongly and noncovalently bound. Plasmid DNA is readily linearized and biotinylated. The C-terminus of streptavidin subunit D has a cysteine that enables covalent immobilization on a functionalized surface by a maleimide-polyethylene glycol (PEG) linker.

To determine the amounts of plasmid DNA needed to produce fusion proteins in amounts sufficient for transferase activity detection, we tested increasing amount of plasmid DNA (containing *At*MUR3-GST) for protein synthesis in a test tube. We then used a [^{14}C]radioactive assay according to (35) using partially degalactosylated nasturtium XyG. Our results indicate that 300-500 ng of plasmid DNA were sufficient to produce fusion proteins for detection of 75 to 95% of

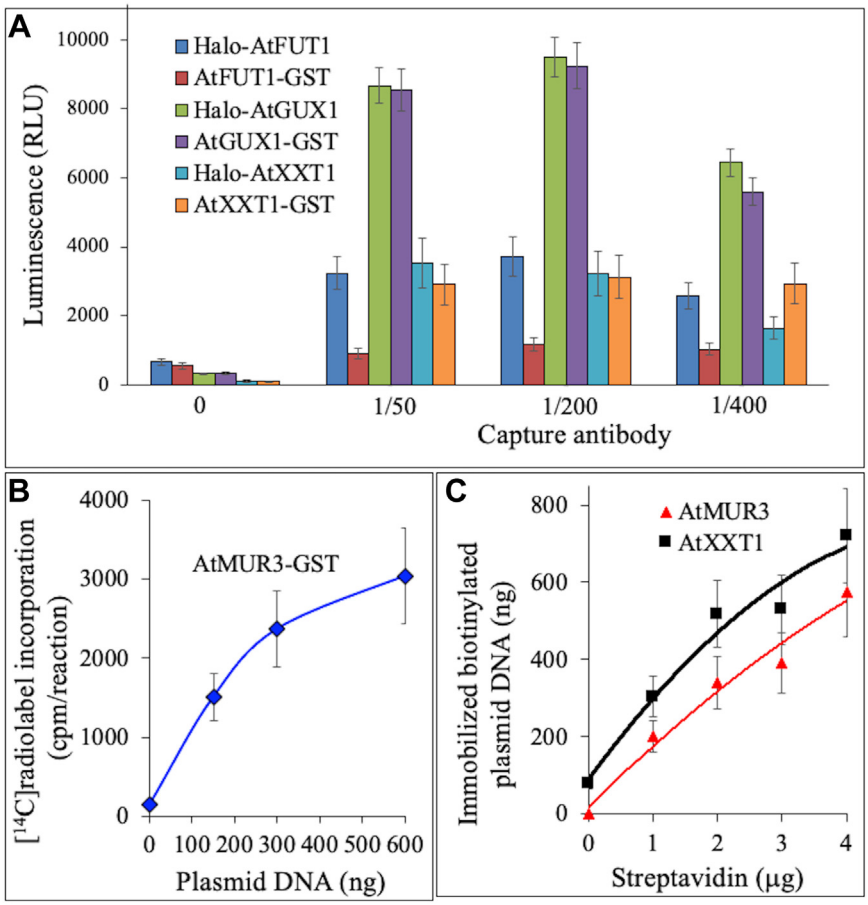

Figure 2. Optimizations of *i*-GT-ray platform for screening of GT activity on microplates. *A*, microwells were coated with three different dilutions of capture antibody (anti-Halo or anti-GST) and the activity of captured GTs was tested using GLO system. *B*, correlation of enzyme activity of *At*MUR3-GST with increasing amount of free plasmid DNA used in the [^{14}C]radioactive assay in a tube. *C*, microwells were coated with various amounts of streptavidin to capture biotinylated plasmid DNA containing *AtXXT1-GST* and *Halo-GUX1* constructs. Two micrograms of streptavidin were necessary to achieve immobilization of ∼500 ng plasmid DNA on the microwells. All assays were performed in duplicate + SD of the means. GTs, glycosyltransferases; *i*-GT-ray, *in vitro* GT-array.

transferase activity obtained in solution (Fig. 2*B*). To immobilize ∼500 ng of biotinylated plasmid DNA, it was necessary to precoat the microwells with 2-3 µg of streptavidin (Fig. 2*C*). For the remaining experiments, GT-arrays were prepared by precoating the microwells with streptavidin (2 µg) and CAb (1/200 dilution). Somewhat unexpectedly, we found that transferase activities were higher when using microwells prepared by precoating with streptavidin and then with CAb, compared to microwells prepared by applying a mixture of streptavidin and CAb. Once all these optimizations were completed, we generated GT-arrays that were successfully used to streamline protein synthesis, immobilization, enzyme assay, and monitoring with GLO system.

i-GT-ray platform can be connected to downstream analytical methods such as MS

One of our goals is to integrate *i*-GT-ray platform with a downstream analysis/detection of the products formed during the transferases reactions. Typically, these products are present in very small amounts and their detection necessitates the use of radioactive NDP sugars as the sugar donors. The use of radioactive materials is not compatible with high-throughput strategy of *i*-GT-ray. Thus, there is a need for an alternative method that is rapid and sensitive to monitor transferase reaction products (*i.e.*, oligosaccharides). We previously optimized a mass spectrometry method called DPS-MS that fits these requirements (34, 38, 39). Thus, we used microplates precoated with biotinylated plasmid DNA and CAb to generate GT-arrays to streamline protein synthesis, immobilization, enzyme assay, and detection of products of Halo-tagged *At*XXT1, *At*FUT6, and *At*GUX1. Arabinotriose (Ara_3, α-L-Araf-(1,5)-α-L-Araf-(1,5)-L-Ara) from arabinan was used as a proxy for an AGP acceptor for *At*FUT6, since AGPs from tobacco cells have arabinotriose side chains with a terminal α(1,5)-linked arabinofuranose (Ara*f*) residue. We showed previously that *At*FUT6 catalyzes Fuc transfer from GDP-Fuc onto Ara*f* residues of these tobacco AGPs (17).

We successfully measured the activity of the three GTs using the GLO system (Fig. 3*A*) and detected the products of the reactions using DPS-MS (Fig. 3, *B–D*). Our results show that Ara_3 is an acceptor for *At*FUT6. The enzyme catalyzed the formation of fucosylated Ara_3 (Fuc-Ara_3), which was detected by DPS-MS as an $[M + Na]^+$ ion at *m/z* 583. The acceptor Ara_3 gives an [M +

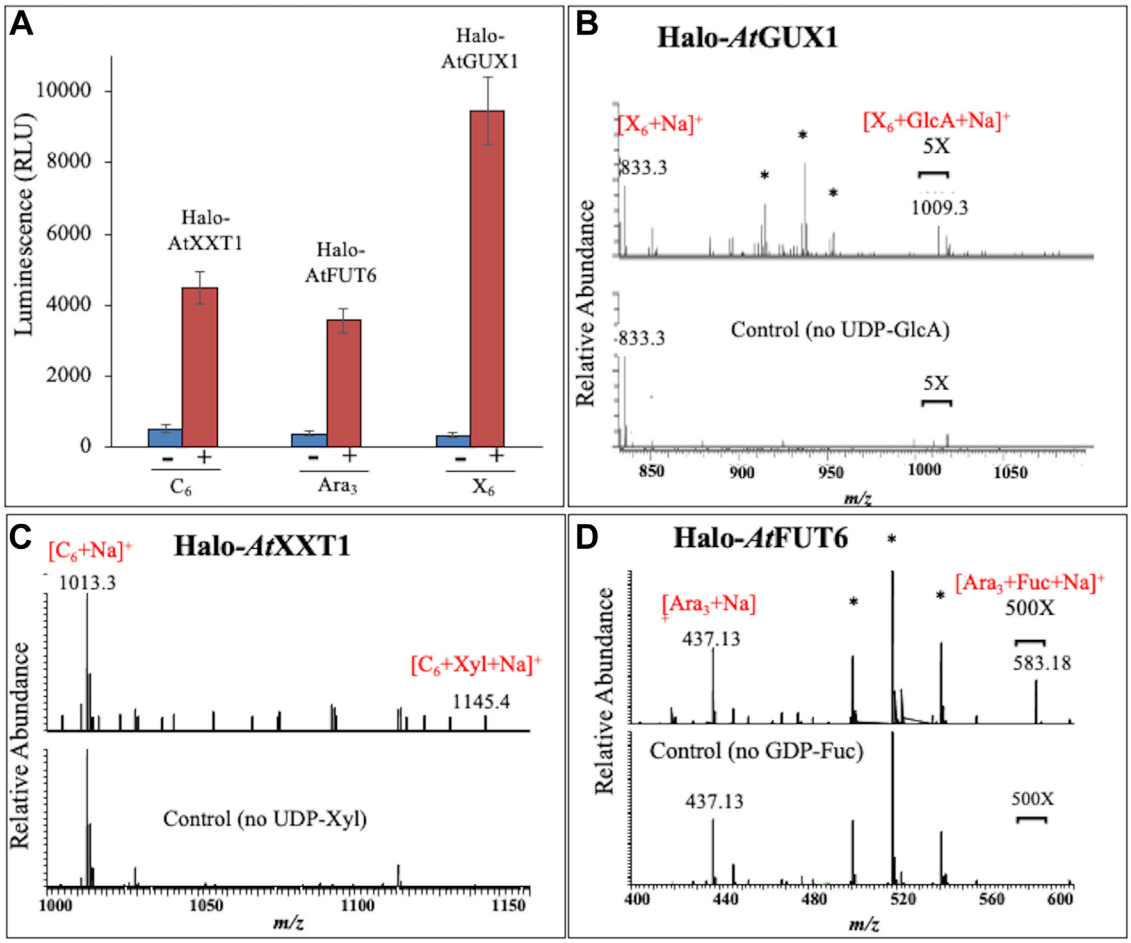

Figure 3. Validation of *i*-GT-ray-DPS-MS platform using Halo-tagged *At*XXT1, *At*FUT6, and *At*GUX1. *A*, transferase activities (in Tris–HCl buffer) of these GTs were measured using GLO system (expressed as luminescence unit, RLU). Assays were performed in triplicates and values are the averages ± SD. DPS-MS was used to detect the products generated by Halo-*At*GUX1 (*B*), Halo-*At*XXT1 (*C*), and *At*FUT6 (*D*). All detections were carried out using 10 μl from transferase reactions performed in microwells. Zoom in spectra are shown as 5X, and 500X. The substrate acceptors used are G_6, Ara_3, and X_6, which stand for cellohexaose, arabinotriose, and xylohexaose, respectively. *Asterix* indicates the peaks are contaminants from the acceptor or donor substrates. DPS-MS detection was performed in duplicate, and representative spectra are shown. DPS-MS, desalting paper spray-mass spectrometry; GTs, glycosyltransferases; *i*-GT-ray, *in vitro* GT-array.

Na]$^+$ ion at *m/z* 437 (Fig. 3*D*). DPS-MS analysis of the products formed by *At*GUX1 reaction with X_6 (*m/z* 833, Fig. 3*B*), gave an ion at *m/z* 1009 corresponding to the formation of GlcA-X_6. Reacting *At*XXT1 with C_6 (*m/z* 1013, Fig. 3*C*) gave an ion at *m/z* 1145 corresponding to the formation of Xyl-C_6. Although the intensities of the product ions were somewhat low, none of the oligosaccharides formed by the GTs were detected in the control reactions lacking donor substrates (GDP-Fuc, UDP-GlcA, or UDP-Xyl). Furthermore, DPS-MS detected these ions with high accuracy (<3 ppm, Table S2). Mass error values lower than 5 ppm is an indication of detection accuracy.

Screening of putative Arabidopsis AtFUTs members of the GT37 family for fucosyltransferase activity

We used our *i*-GT-ray platform to screen seven (of the ten) Arabidopsis family GT37 FUTs with no established function for their activity toward five acceptors. Non-fucosylated RG-I(*mur1*) and RG-II(*mur1*) acceptors were isolated from the cell walls of Arabidopsis *mur1-1* mutant plants. This mutant is unable to produce GDP-L-Fuc as it carries a mutation in the *GDP-mannose 4,6-dehydratase* (*GMD2*) gene (9, 40, 41). The Fuc and MeFuc residues in RG-II(*mur1*) are partially replaced with L-Gal and L-MeGal (40, 42). Thus, we used as an alternative acceptor, a deesterified RG-II monomer from celery, that had been treated with glycosyl hydrolases that specifically remove the MeFuc and Ara*p* from side chain B and the L-Gal from side chain A (RG-II(-L-Gal,-Fuc), Fig. 5 for structures).

Arabidopsis has ten members in the GT37 family and seven of them are currently annotated as putative FUTs with no known enzyme activity. All *At*FUTs were predicted to have one transmembrane domain, except *At*FUT8 and *At*FUT9, which were predicted to have two transmembrane domains and *At*FUT10 predicted to be secreted soluble protein. *At*FUT1 and *At*FUT6 fucosylate XyG and AGP, respectively, and were used as positive controls. We performed 100 assays using *i*-GT-ray platform with GLO assays to screen the nine *At*FUTs against five non-fucosylated potential acceptors with negative controls (no acceptors added) to determine whether the *At*FUTs have hydrolysis activity of GDP-Fuc. None of the putative *At*FUTs hydrolyzed GDP-Fuc in the absence of acceptors. *At*FUT2, *At*FUT5, and *At*FUT10 showed a more than

three-fold increase in the activity for RG-I(*mur1*) acceptor compared to the control (Fig. 4*A*) *At*FUT8 acted on celery RG-II(-L-Gal,-MeFuc), whereas RG-II(*mur1*), in which side chain A is largely truncated to a tetrasaccharide (42) was not an acceptor for *At*FUT8. The controls *At*FUT1 and *At*FUT6 acted on TXyG and Ara_3, respectively as expected (Fig. 4*A*). Fucose is α(1,2)-linked to Gal in the type-I AG of RG-I whereas MeFuc is α(1,2)-linked to Gal in side chain B of RG-II (43–45). Since all FUTs from GT37 family thus far characterized catalyze α(1,2) linkages in various plant cell wall polysaccharides, we anticipated that these *At*FUTs would also catalyze α(1,2) linkages on RG-I(*mur1*) and RG-II(-L-Gal,-Fuc).

To further our understanding of RG-II fucosylation, we used the celery monomer lacking the MeFuc and Ara*p* of side chain B or the celery monomer lacking the L-Gal of side chain A as acceptors (Fig. 5 for structure). The presence of L-Gal in side chain A strongly reduced the ability of *At*FUT8 to act on the RG-II(+L-Gal,-Fuc) acceptor (Fig. 5). *At*FUT8 was able to act on RG-II(-L-Gal,+MeFuc) acceptor (Fig. 5). However, the RG-II isolated from the walls of the *atfut8* single mutant (SALK_010981) existed predominantly as the dimer (Fig. S4) and had a monosaccharide composition similar to RG-II from WT plants (Tables S3 and S4).

Screening of putative rice OsFUTs members of the GT37 family for fucosyltransferase activity

No fucosyltransferase activity has been demonstrated for any of the grass members of family GT37. To address this, we screened 15 rice FUTs for activity toward the same five substrates used with the Arabidopsis FUTs. With the exception of Os02g0763900, which is predicted to be soluble protein with no secretion signal peptide, all the other putative *Os*FUTs are predicted to be type II membrane proteins.

We used Halo-tagged versions of the rice *Os*FUTs, since all N-terminal Halo-tagged *At*FUTs were active. *At*FUT1 and *At*FUT6 were included as positive controls as were controls lacking the acceptors to determine if the *Os*FUTs just hydrolyze GDP-Fuc. None of the putative *Os*FUTs hydrolyzed GDP-Fuc in the absence of acceptors. As indicated in Figure 6*B*, *At*FUT1 and *At*FUT6 had the expected XyG-FUT and Ara_3-FUT activities, respectively. *Os*FUTs (Os02g0763200, Os02g02763900, Os02g0764200 (*Os*MUR2), Os04g0449100, and Os06g0212100) were active against TXyG (Fig. 6*B*). *Os*MUR2 is annotated as a XyG-FUT (20), and our data confirm its enzyme activity *in vitro*. Os02g0763200 acted on TXyG *in vitro*, but did not restore fucosylation of XyG in the *Atfut1* mutant (20). It is not known if Os02g02763900, Os04g0449100, and Os06g0212100, which also showed activity on TXyG, can complement the *Atfut1* mutant. Neither Os02g0764400 nor Os06g0211600 showed activity on TXyG *in vitro* and they did not complement the *Atfut1* mutant (20). Therefore, rice may have only one true XyG-FUT (*Os*MUR2). The remaining *Os*FUTs may fucosylate other cell wall polymers but have broad acceptor substrates *in vitro* and thus show activity on TXyG. It is not known if these *Os*FUTs use GDP-L-Gal as well as GDP-Fuc as donor substrates, as has been demonstrated for *At*FUT1 (46).

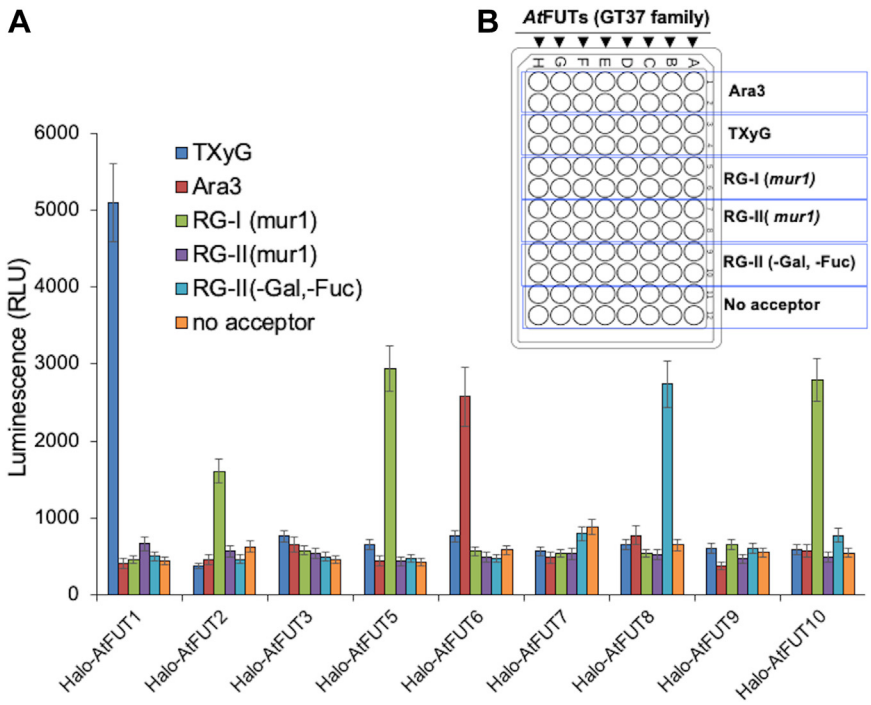

Figure 4. Fucosyltransferase activity of nine Arabidopsis *At*FUTs from GT37 family on *i*-GTray platform. *A*, N-terminal Halo-tagged *At*FUT1, *At*FUT2, *At*FUT3, *At*FUT5, *At*FUT6, *At*FUT7, *At*FUT8, *At*FUT9, and *At*FUT10 were synthesized and immobilized on microwells and their activity was monitored in the presence or absence of the acceptor and GDP-Fuc using GLO system. Acceptors used are non-fucosylated rhamnogalacturonan (RG) from *mur1* mutant [RG-I(mur1) and RG-II(*mur1*)], deesterified celery RG-II monomer lacking Ara*p* and MeFuc of side chain B and L-Gal of side chain A [RG-II(-Gal,-Fuc)], arbinotriose (Ara_3), and tamarind xyloglucan (TXyG). Halo-tagged *At*FUT1 and AtFUT6 were used as positive controls. *B*, the layout for fucosyl transfer assays on *i*-GTray platform. A total of 100 FUT assays were performed in duplicates and values are the averages ± SD. FUT, fucosyltransferase; *i*-GT-ray, *in vitro* GT-array; RG, rhamnogalacturonan.

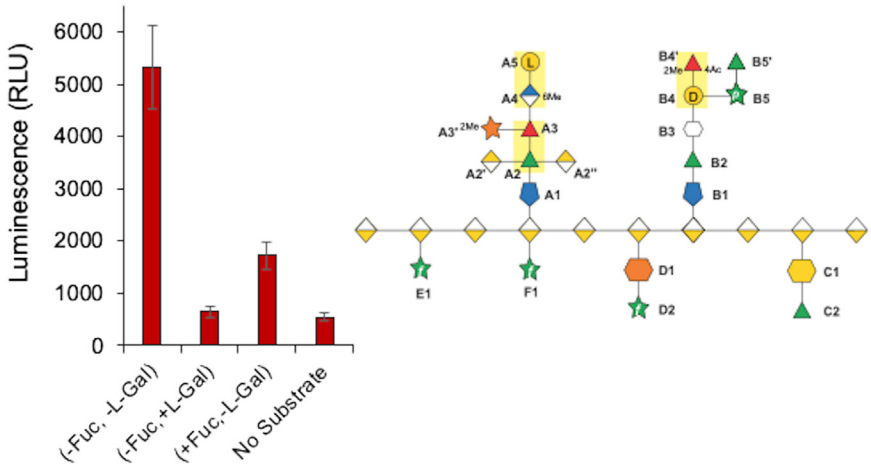

Figure 5. Activity of *At*FUT8 on modified rhamnogalacturonan (RG)-II monomers from celery. The acceptors used are deesterified RG-II monomers lacking Ara*p* (B5 in the illustration) and MeFuc (B4′) of side chain B and L-Gal of side chain A (A5 in the illustration) [RG-II(-L-Gal,-Fuc)], deesterified RG-II lacking Ara*p* and MeFuc of side chain B but has unchanged side chain A [RG-II(+L-Gal,-Fuc)], RG-II lacking L-Gal of side chain A with unchanged side chain B [RG-II(-L-Gal,+Fuc)]. Illustrations of the RG-II structure is indicated on the right using standard drawing symbols of monosaccharides (61). The position of the Fuc (*red triangle*) in the acceptor are highlighted in *yellow boxes*. RG, rhamnogalacturonan.

Four *Os*FUTs (Os02g0764200, Os06g0211600, Os06g0211700, and Os06g0212600) could act on Ara_3, with Os02g0764200 (*Os*MUR2), Os06g0211700, and Os06g0212100 having the highest activity (Fig. 6*B*). Surprisingly, *Os*MUR2, which is a XyG-FUT, could also act on Ara_3 demonstrating that *Os*MUR2 can recognize two completely different acceptors *in vitro*. It is not known if *Os*MUR2 can fucosylate AGP *in vivo* (for example, by introducing *OsMUR2* gene in Arabidopsis *atfut4*/*atfut6* double mutant background, which lacks Fuc in its AGPs (47). None of the rice *Os*FUTs showed activity toward RG-I(*mur1*) and RG-II(-L-Gal,-Fuc) acceptors (Fig. 6*B*).

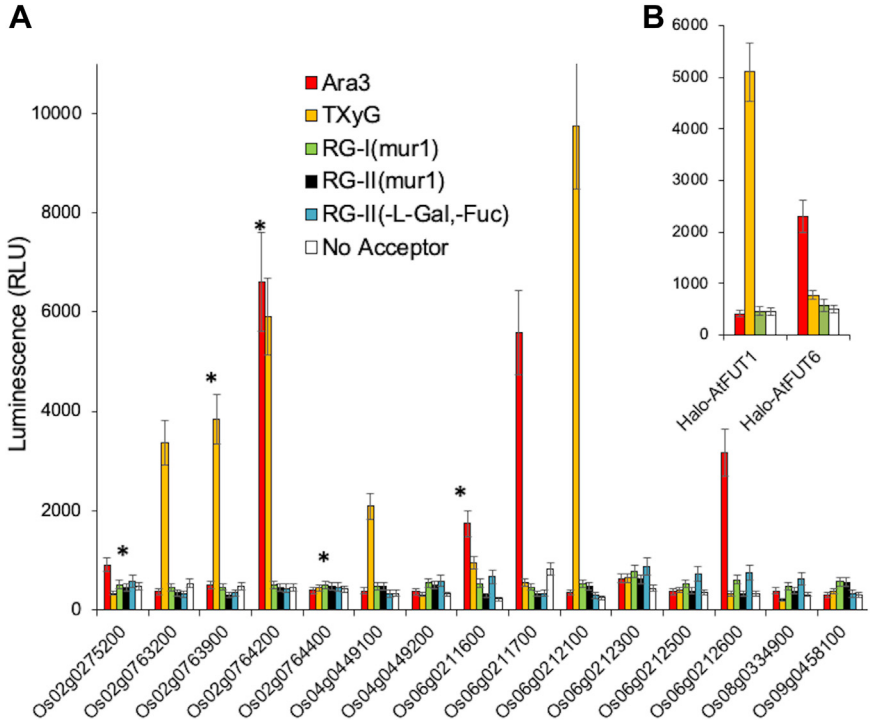

Figure 6. Fucosyltransferase activity of 15 putative rice *Os*FUTs members of the GT37 family on *i*-GT-ray platform. *A*, N-terminal Halo-tagged GTs were synthesized and immobilized on microwells and their activity was monitored in the presence GDP-Fuc and in the presence or absence of the acceptor using GLO system. Acceptors used are nonfucosylated rhamnogalacturonan (RG) from *mur1* mutant [RG-I(mur1) and RG-II(*mur1*)], deesterified celery RG-II monomers lacking Ara*p* and MeFuc of side chain B and L-Gal of side chain A [RG-II(-L-Gal,-Fuc)] (see illustration in Fig. 5), arbinotriose (Ara_3), and tamarind xyloglucan (TXyG). *B*, Halo-tagged *At*FUT1 and *At*FUT6 were used as positive controls. A total of 180 assays were performed (including duplicates) and values are the averages ± SD. "*" indicates these FUTs were previously tested by overexpression in Arabidopsis *axy2.2/fut1/mur2* mutant background (20). FUT, fucosyltransferase; GTs, glycosyltransferases; *i*-GT-ray, *in vitro* GT-array; RG, rhamnogalacturonan.

Discussion

Determining the enzyme activities of new GTs will improve our understanding of the mechanisms of plant cell wall polysaccharides biosynthesis and the physiological role of a particular sugar/polymer in plant development and fitness. However, determining GTs enzyme activities *in vitro* is time-consuming and the least adapted to large-scale screening of GTs (48). This work describes the implementation of a powerful screening platform (*i*-GT-ray) based on NAPPA method. *i*-GT-ray simplifies the testing of enzyme activity *in vitro* of many GTs simultaneously (at lower costs and in less time). Our platform uses GT-arrays, generated by precoating microplates with plasmid DNA and CAb (anti-tag antibody). GT-arrays can be stored or used immediately for *in vitro* transferase assays. Four benchmarked nonprocessive GTs (*At*FUT1, *At*XXT1, *At*GUX1, and *At*MUR3) were used to optimize the amounts of plasmid DNA and CAb needed on the microplates and to identify a buffer suitable for the GTs. We were able to streamline the production of tagged GTs directly from plasmid DNA, their capture by the immobilized CAb, performing enzyme assays, and detection of the generated products in a single experiment and in a shorter time (48 h) compared to heterologous expression of GTs and purification. Importantly, we demonstrated that GST- or Halo-tagged GTs can be produced in a soluble and active form (in the absence of detergent) using cell-free IVTT systems. Our *i*-GT-ray screening platform has several advantages for GTs activity testing *in vitro*. Traditionally, GT must be expressed in heterologous systems and then purified before *in vitro* assays (may take at least 1 week). These procedures cannot be adapted to high-throughput. In *i*-GT-ray, cell-free production of GTs and immobilization on the surface of the microwells combines production and purification steps, which saves time (∼48 h). The transferase reactions can then be monitored directly on microplates using the GDP/UDP-GLO systems. The products of these reactions can be detected directly through DPS-MS, provided a suitable acceptor is available. All these processes can be performed in a single experiment. The *i*-GT-ray platform overcomes the problem of NDP-sugar donor interconversion (49), which often occurs when using Golgi-enriched membranes (or solubilized and partially purified GTs) as enzyme sources. Such interconversion typically results in the formation of multiple products, which complicates analysis of the reaction products.

For validation, *i*-GT-ray platform was used to screen 22 FUTs from GT37 family (seven Arabidopsis and 15 rice putative FUTs) for activity toward five non-fucosylated potential acceptors, including TXyG, Ara_3, RG-I, and RG-II. None of these FUTs have known acceptor/donor substrates, although members of family GT37 are predicted to catalyze the addition α(1,2)-linked Fuc residues onto plant cell wall glycans. Our data suggest that *At*FUT2, *At*FUT5, and *At*FUT10 are RG-I-FUTs since they acted on the RG-I(*mur1*) acceptor, but not on WT RG-I. *At*FUT8 may fucosylate RG-II, as it acted on celery RG-II(-L-Gal,-MeFuc), but not on RG-II(*mur1*) acceptor because the B side chain MeFuc residues is replaced with L-MeGal (40). Interestingly, we observed no activity of *At*FUT8 toward RG-II(+L-Gal, -MeFuc) acceptor, which has the terminal L-Gal in side chain A but no MeFuc in side chain B, suggesting that the addition of terminal sugars in side chains A and B may proceed in an ordered manner (Fuc first and then L-Gal), and the order of synthesis of side chain A might be dependent on order of synthesis of side chain B. We also observed that *At*FUT8 had some activity toward the RG-II(-L-Gal,+MeFuc) acceptor, which has the terminal MeFuc in side chain B but no terminal L-Gal of side chain A. Thus, *At*FUT8 may transfer Fuc to the GlcA residue of the side chain A. This was surprising because there are no reports that a terminal L-Gal is replaced by L-Fuc on side chain A of naturally occurring RG-II. Furthermore, an Arabidopsis galactosyltransferase (L-GalT called Cdi, At1g64980) responsible for the addition of L-Gal to GlcA in side chain A was recently identified through genetic analysis of *cdi* mutant (50). RG-II from this mutant lacked the terminal L-Gal. Interestingly, while *At*FUT8 showed activity on RG-II acceptor used *in vitro*, the monosaccharide composition and dimerization status of RG-II from *atfut8* mutant plants were similar to WT plants (Fig. S4, Tables S3, and S4). One possible explanation is that *At*FUT8 may have broader acceptor substrates (promiscuity) *in vitro*, but may have a different acceptor substrate specificity *in vivo*. Thus, the RG-II-FUT that adds the terminal Fuc/MeFuc of side chain B may be from a different GT family or a family not yet identified. Promiscuity toward acceptor substrates was also observed for *At*FUT1, as analysis of XyG from root hair of Arabidopsis *atfut1* mutant led Peña *et al.*, (2012) (51) to conclude that *At*FUT1 may be also responsible of the fucosylation of the GalA residues of root hair XyG.

Our screening of putative rice *Os*FUTs showed that five *Os*FUTs acted on TXyG. *Os*MUR2 (Os02g0764200) has been previously assigned XyG-FUT function through genetic complementation of *axy2.2/fut1/mur2* mutant plants that lack fucosylated XyG (20). Our data provide direct evidence that *Os*MUR2 has XyG-FUT activity *in vitro*. Three other putative *Os*FUTs (indicated by "*" in Fig. 6) were also tested in the same genetic complementation experiment but failed to rescue the chemotype, and one of those *Os*FUTs (Os02g0763200) was active on TXyG in our platform (Fig. 6), but did not complement the *axy2.2/fut1/mur2* mutant, which also suggests that Os02g0763200 might be a FUT for a different cell wall polymer *in vivo*. *Os*MUR2 was found to be also active on Ara_3 (Fig. 6). In addition to *Os*MUR2, three additional putative *Os*FUTs (Os06g0764200, Os06g0211700, and Os06g0212600) could also act on Ara_3. Recently, *At*FUT7 was assigned AGP-FUT activity (52), but this *At*FUT did not show AGP-FUT activity in our screening platform. Taken together, these findings suggest that several FUTs from GT37 family have promiscuity toward acceptor/donor substrates *in vitro*. Nevertheless, if this promiscuity does exist it must be controlled *in vivo*. One possibility could be simply a tight regulation at the gene expression level to coincide with the presence of the appropriate acceptors. Another possibility is the presence of endogenous cofactors (in Golgi or ER) that

allow FUTs to acquire substrate specificity. The structural conformation of the acceptor present during the formation of the polymer may also have a role in controlling the type of glycosidic bond that can be formed (53).

Perhaps the most intriguing finding is that none of the rice enzymes acted on non-fucosylated RG-I(*mur1*) and RG-II(-L-Gal,-Fuc) acceptors. The absence of FUT activity on RG-I(*mur1*) in rice is in agreement with previous reports indicating that RG-I in the Poaceae is not fucosylated (42, 45). However, the possibility remains that the non-fucosylated RG-I(*mur1*) acceptor used in this study may lack the appropriate fucosylation sites for rice RG-I-*Os*FUTs. On the other hand, the fact that none of putative rice *Os*FUTs acted on RG-II(-L-Gal,-Fuc) acceptor was surprising considering that the structure of RG-II is largely conserved in vascular plants (42, 54). Furthermore, there are still six putative rice *Os*FUTs (Os02g0275200, Os02g0764400, Os04g0449200, Os06g0212300, Os08g03 34900, and Os09g0458100) and two putative Arabidopsis *At*FUTs (*At*FUT3 and *At*FUT9) with unknown enzyme activity. The implication of this result is that either (i) some fucosylated polymers (to be identified) might be present in the cell wall at very low amounts, and the appropriate acceptors for these polymers are not currently available; (ii) these FUTs may require additional factors to fucosylate some of the acceptors used in this work; (iii) these FUTs may use a different donor substrate (other than GDP-Fuc); or (iv) the lack of activity of these tagged GTs is due to misfolding, which we believe unlikely.

In conclusion, we have developed a platform for high-throughput screening of GT activities. The platform allowed the generation of GT-arrays that can be used to screen substrate specificity for putative GTs whose functions are currently unknown or incompletely characterized. However, it is important to emphasize that *i*-GT-ray should be considered as a first step for rapid screening of GTs, as the platform alone does not provide information about the type of linkage (alpha *versus* beta) nor about the position of the linkage (between sugars). Therefore, the platform developed can contribute in facilitating the progress in determining the biochemical function of GTs in plants and other organisms and has the potential to be extended to enzymes other than GTs (*i.e.*, hydrolases). The platform has some limitations such as possible misfolding of some proteins during the binding to microplate or no production of the proteins. The next challenge would be to assemble functional complexes of multiple GTs on GT-arrays that can produce full polymers *in vitro*. Furthermore, since we optimized the binding of DNA plasmid to microwell surface, it would be possible to adapt this platform as an additional method to investigate DNA–protein interactions associated with transcription factors for plant cell wall biosynthesis. Using *i*-GT-ray platform, we presented the first testing of enzyme activity of rice and Arabidopsis FUTs of the GT37 family against five non-fucosylated acceptor substrates, which expanded our view of the fucosylation landscape of plant cell wall polysaccharides in a dicot and a grass.

Experimental procedures

Chemicals and plant materials

Manganese (II) chloride, magnesium chloride, potassium chloride, sodium bicarbonate, detergents, and DOWEX 1X8-100 resin (Cl) were obtained from Sigma-Aldrich. HPLC-grade Tris, Hepes, acetic acid, potassium phosphate, formic acid, scintillation liquid, Immobilon membrane, SuperSignal West Femto Maximum Sensitivity Substrate, PureLink RNA Mini Kit, streptavidin, and biotin were from Thermo Fisher Scientific. GST was from GenScript. GDP-[^{3}H]Fucose (299.7 GBq/mmol), GDP-[^{14}C]Mannose (5.123 GBq/mmol), UDP-[^{14}C]Xylose (7.141 GBq/mmol) and UDP-[^{14}C]Glucuronic acid (9.213 GBq/mmol) were purchased from PerkinElmer Life Sciences. UDP-[^{14}C]Galactose (1.85 GBq/mmol) was purchased from American radiolabeled chemicals Inc. UDP-Xylose was purchased from CarboSource (University of Georgia). GDP-fucose and UDP-glucuronic acid were purchased from Sigma-Aldrich. GDP or UDP-GLO glycosyltransferase assay, Halo-GST tag fusion protein, and protein expression kit (TNT Quick Coupled Transcription/Translation System) were purchased from Promega. 1-Step Human Coupled IVT Kit was purchased from Invitrogen. β-galactosidase, tamarind xyloglucan (TXyG), cellohexaose (C_6), xylohexaose (X_6), and arabinotriose (Ara_3) were purchased from Megazyme. X-ray film was purchased from Research Products International Corp. *pCR8/GW/TOPO* TA Cloning Kit and Gateway LR Clonase II enzyme mix kit were purchased from Invitrogen. The expression vector *pJFT7_nHALO* and *pANT7_cGST* were purchased from DNASU Plasmid Repository housed at The Biodesign Institute/Arizona State Universitye. NucleoBond Xtra Midi kit was purchased from Macherey-Nagel. A 96-well microplate (clear, flat bottom, half area, high binding, and polystyrene) was purchased from Corning. Anti-GST antibody was purchased from GE HealthCare Life Sciences, and anti-Halo antibody was purchased from Promega. Secondary mouse anti-goat immunoglobulin G (IgG) horseradish peroxidase (HRP) conjugated was purchased from Santa Cruz Biotechnology and secondary anti-rabbit IgG HRP conjugated was purchased from Promega. One-step ultra TMB-ELISA and sulfuric acid was purchased from Thermo Fisher Scientific.

Cloning of GT genes

Full-length complementary DNA (cDNA) clones of *AtFUT1 (At2g03220), AtFUT6 (At1g14080), AtXXT1 (At3g62720), AtXXT2 (At4g02500), AtXXT5 (At1g74380), AtGUX1 (At3g18660)*, and *AtMUR3 (At2g20370)* were obtained from the Arabidopsis Biological Resource Center (ABRC) DNA Stock Center in the *pDONR223* vector. The cloning steps are as follow: full-length protein coding sequences were amplified using gene-specific primers (Table S5) and HiFi polymerase, resulting in one PCR products with a stop codon and one without a stop codon. Both forms of PCR products were then cloned into the *pCR8/GW/TOPO* vector following the manufacturer's protocol. Sanger sequencing was used to determine

the correct orientation of the genes and confirm the absence of any mistakes in the sequences. The *pCR8/GW/TOPO* vector containing the PCR product with the stop codon was transferred to the *pJFT7_nHALO* expression vector using the Gateway LR Clonase II enzyme mix kit (Invitrogen) to create an N-terminal Halo-tagged fusion protein. The PCR product without a stop codon was transferred to the *pANT7_cGST* expression vector, generating a GST-tagged fusion protein using the Gateway LR Clonase II enzyme mix kit (Invitrogen). Gateway LR reactions were carried out in 8 μl total volume containing 150 ng of destination vector (either *pANT7-cGST* or *pJFT7-nHalo*), 150 ng of entry vector (*pDONR223* or *pCR8/GW/TOPO* vectors containing the GT genes) and 2 μl of LR Clonase II enzyme mix. The Gateway LR reactions were performed according to the manufacturer's instructions.

For the 15 rice genes from GT37 family, four clones were obtained from Dr Zeng's lab (Zhejiang A&F University, Sino-Australia Plant Cell Wall Research Centre, and State Key Laboratory of Subtropical Silviculture). The remaining rice genes were cloned *via* RT-PCR. mRNAs were extracted from one month-old rice plants (100 mg). cDNAs were synthesized from mRNAs using Superscript III reverse transcriptase according to the manufacturer's instruction (Life Technologies). cDNAs for FUT genes were amplified using gene-specific primers (Table S5) and HiFi polymerase. The PCR products (with and without a stop codon) were cloned into *pCR8/GW/TOPO* vector before transfer to *pANT7-cGST* or *PJFT7-nHalo* vectors using gateway technology as described above. Large amount of purified plasmid (mg) was prepared from 200 ml bacteria cultures (LB broth at 37 °C for overnight) using the NucleoBond Xtra Midi kit (Macherey-Nagel). All rice GT37 FUT genes were cloned except *Os10g0125100*, which was the only FUT annotated as a *O*-fucosyltransferase-like protein and *Os06g0212300*, which failed to amplify.

Preparation of GT-arrays: binding of plasmid DNA and CAb to microplates

Microplates with clear, flat bottom, half area, and high binding polystyrene (Corning Inc) were coated with streptavidin (2 μg in 50 μl 50 mM sodium bicarbonate, pH 9.6) for overnight at 4 °C. Unbound streptavidin was removed by washing with 10 mM phosphate buffered saline (PBS) (3 times, 10 min each). Linearized and biotinylated plasmid DNA (1 μg) in 10 mM (PBS, 50 μl) was applied to each well and the plate kept for at least 4 h at 20 °C with shaking at 250 rpm. Unbound plasmid DNA was removed by washing 3 times (10 min each) with10 mM PBS. The amounts of attached plasmid DNA was estimated using the AccuBlue NextGen dsDNA quantitation kit (Biotium). Our protocol resulted in the attachment of ∼500 ng plasmid DNA to the microwell of a microplate.

The plasmid-precoated microplates were incubated overnight at 4 °C with 50 μl of 50 mM sodium bicarbonate buffer, pH 9.6 containing anti-GST or anti-Halo antibody at various dilutions (as specified in the text). After incubation, the wells were washed with PBS buffer (3 times, 10 min each) to remove unbound CAb, and then microwells were blocked for at least 6 h at 4 °C with 5%(w/v) fat-free dry milk in PBS. The microplates can be used immediately for protein synthesis and capturing or stored at 4 °C for up to 60 days.

Linearization and biotinylation of plasmid DNA

To generate linearized and biotinylated DNA, 60 μg of plasmid DNA was linearized using *Pfo*I and freeze-dried. The pellet was dissolved in 10 μl water and then 7.5 μl (40–50 μg) of the linearized plasmid DNA solution was mixed with ∼1.25 mg (6.52 μmol) of 1-ethyl-3-[3-dimethylaminopropyl] carbodiimide hydrochloride. Biotin hydrazide (0.25 mM in 0.1 M imidazole, 5 μl) was immediately added and the mixture vortexed, and 20 μl of 0.1 M imidazole was added before incubation overnight at 37 °C. The nonreacted 1-ethyl-3-[3-dimethylaminopropyl] carbodiimide hydrochloride and its by-products were removed using a spin desalting column (Zeba Spin Desalting Column) using 10 mM PBS containing 150 mM NaCl and 10 mM EDTA. The biotinylated plasmid DNA can be stored at −80 °C until use.

In vitro *production of GT proteins in tubes and on microplates*

Tagged GT proteins were produced using 25 μl TNT Quick Coupled Transcription/Translation System (Promega) or 1-Step Human Coupled IVT Kit (Thermo Fisher Scientific) either in 1.5 ml Eppendorf tubes using 1 μg GT plasmid DNA (two-step approach) or on 96-well microplates (one-step approach). The reactions were incubated for 4-6 h at 30 °C without shaking.

In the two step approach, the tagged GT proteins were synthesized in tubes using one of the IVTT systems and the synthesized fusion proteins were applied to microplates that were precoated with CAb (dilutions used are specified in text). The capturing of tagged GT proteins by CAb was carried out as follows: tagged proteins (usually in 25 μl) were mixed with 5% (w/v) fat-free milk in PBS buffer in 1:3 ratio (final volume 100 μl), and each well receives 50 μl of this mixture. After incubation overnight at 14 °C with shaking at 250 rpm, non-captured tagged GT proteins were removed by washing with PBS buffer (3 times, 10 min each). The microplates having tagged proteins attached to the CAb can be used immediately for transferase assays or stored sealed at 4 °C for up to 60 days.

In the one-step approach, tagged GT proteins were produced directly on microplates using 50 μl of one of the IVTT systems according to the manufacturer's recommendations and microplates incubated for 4 to 6 h at 30 °C. The synthesized fusion proteins were allowed to attach to CAb by incubation for at least an additional 4 h at 14 °C with shaking at 250 rpm. Unbound fusion proteins were removed by washing with PBS buffer (3 times, 10 min each). These microplates, which are now precoated with "fusion protein-CAb" complex (in addition to "plasmid DNA-streptavidin" complex) can be used immediately for transferase assays (see section below) or stored at 4 °C for up to a week (depending on the stability of the GT).

Immunoblotting analysis

To determine the efficiency of protein expression *in vitro*, 4 μl of expression reaction were analyzed by Western blotting. The produced proteins were separated on SDS-polyacrylamide

gels and then transferred onto Immobilon membranes (Thermo Fisher Scientific) using the mini-protein tetra cell system (Bio-Rad). After transfer, the membranes were blocked overnight at 4 °C with 5% (w/v) fat-free dry milk in PBS. The membranes were incubated for 1 to 3 h with the primary antibody (anti-GST or anti-Halo) at a 1:10,000 dilution in PBS containing 5% (w/v) fat-free milk and 0.05% (v/v) Tween 20. After washing (three times, 10 min each) with PBS containing 0.05% (v/v) Tween 20 to remove unbound primary antibody, the membranes were kept for 1 h at room temperature with the secondary antibody (mouse anti-goat IgG or anti-rabbit IgG fused to HRP at a 1:15,000 dilution in PBS containing 5% (w/v) fat-free milk with 0.05% (v/v) Tween 20. Excess of secondary antibody was removed by several washes (5–8 times, 15 min each) with PBS containing 0.05% (v/v) Tween 20. The presence of the fusion protein was detected using SuperSignal West Femto Maximum Sensitivity Substrate (Thermo Fisher Scientific) and exposure to X-ray film (Research Products International Corp) according to the manufacturer's recommendation. In some experiments, the detection of the bands was performed using ChemDoc MP (Bio-Rad).

Transferase assays

Substrates acceptors used in this work were tamarind xyloglucan (TXyG), cellohexaose (C_6), xylohexaose (X_6), arabinotriose (Ara_3), RG-I(*mur1*), and RG-II(*mur1*) both prepared from Arabidopsis *mur1-1*. RG-II(-L-Gal,-Fuc), RG-II(+L-Gal,-Fuc), and RG-II(-L-Gal,+Fuc) were prepared by treating de-esterified celery RG-II with chains A- and B-specific exoglycanases. Nasturtium seed XyG was degalactosylated by treatment with β-galactosidase from *Aspergillus niger* (E-AGLAN, Megazyme) as described in (35). Non-fucosylated AGPs were prepared from the *fut4/6* Arabidopsis double mutant (47, 55) or from tobacco BY2 cell culture, which produce AGPs lacking terminal Fuc (17).

Nonradioactive assays in 50 µl reaction volume on microplates using NDP-sugars and acceptors according to published data. Transferase activity was monitored by measuring the release of UDP or GDP using the UDP-GLO or GDP-GLO glycosyltransferase assay, respectively, (Promega) according to the manufacturer's protocol. The relative luminescence signal was measured with a Synergy/HTX multi-mode reader (BioTek). Reaction products were also analyzed by DPS-MS (34). The reactions were collected from the microwells, stopped by adding 0.3 ml water, freeze-dried, and then solubilized at the desired concentration for DPS-MS. All the assays were performed in technical duplicates.

Radioactive assays were performed as indicated for nonradioactive assays, except that the appropriate NDP-[^{14}C] sugars were used. If the acceptors were oligosaccharides (*i.e.*, for testing *At*GUX1, *At*XXT1), excess of unused NDP-[^{14}C] sugars were removed either by chelation with DOWEX 1X8-100 resin (Cl) 1:1 (v/v) or by TLC, according to the published work (56, 57). If the acceptors were polysaccharides (*i.e.*, for testing *At*FUT1 and *At*MUR3), the reactions were collected from the wells in a tube, and 1 ml of cold 70% ethanol was added and kept overnight at 4 °C. The precipitate that formed was collected by centrifugation and the pellet rinsed five times with 1 ml of cold 70% ethanol to remove excess of NDP-[^{14}C] sugars. The dried pellets were resuspended in 0.3 ml water and mixed with 3-5 ml of liquid scintillation solution. The radioactivity was measured as cpm using a LS 6500 multi-purpose scintillation counter (Beckman Coulter).

Acid hydrolysis and monosaccharide composition analysis

Solutions of polysaccharide (∼250 µg) in 2M TFA (350 µl) were kept for 1.5 h at 120 °C. The acid was then removed under a flow of air. The released monosaccharides were converted to their alditol acetate derivatives and analyzed by GC-MS as described in (58)

Isolation of RG-I and RG-II

RG-I and RG-II was solubilized from the destarched alcohol insoluble residue of Arabidopsis leaves and flowers and from celery petioles using endopolygalacturonase (M1, Megazyme 5 units/g) as described in (58) The RG-I and RG-II was then isolated using Superdex G-75 size-exclusion chromatography. Neutral carbohydrate contaminants of RG-I and RG-II were removed using DEAE-Superose anion-exchange chromatography as described in (58)

Enzyme treatments of RG-II

A solution of celery RG-II (5 mg/ml) in 0.1 M HCl was kept for 1 h at room temperature to hydrolyze the borate diester and generate the monomer. The solution was then dialyzed (3500 molecular weight cutoff) against deionized water. An equal volume of cold 200 mM NaOH was added and the mixture kept for 16 h at 4 °C to deesterify the RG-II. The solution was adjusted to pH 5 by dropwise addition of glacial acetic acid, dialyzed (3500 molecular weight cutoff) against deionized water, and freeze dried.

Recombinant 2-*O*-methyl α-L-fucosidase (BT0984; MeFucase), α-L-arabinopyranosidase (BT0983; Arapase), and α-L-galactosidase (BT1010; L-Galase) were obtained from NZYtech. Solutions of the de-esterified monomer (6 mg) in 50 mM NaOAc, pH 5.2 (500 µl), were treated for 24 h at 37 °C with the L-Galase (10 µg), the Arapase (10 µg), and the MeFucase (10 µg). A separate solution of celery monomer was also treated with the Arapase and MeFucase. The reactions mixtures were chromatographed on a Superdex 75 size-exclusion chromatographic column and the monomeric RG-II collected. The solutions were repeatedly freeze dried to remove the ammonium formate. Portions of each product (∼250 µg) were then treated for 1 h with 0.1 M TFA at 80 °C to release side chains A and B or for 16 h at 40 °C with 0.1 M TFA to preferentially release side chain B. The acid was removed under a flow of warm air and the residue dissolved in water (∼1 mg/ml). MALDI-TOF-MS analysis of the products confirmed that only the expected glycoses had been removed from side chains A and B.

Desalting paper spray-mass spectrometry

A high-resolution Q Exactive Orbitrap mass spectrometer (Thermo Fisher Scientific) was used throughout this study.

The commercial electrospray ionization ion source was removed to accommodate DPS. Data analysis was acquired by Thermo Xcalibur (3.0.63). The filter paper was cut into triangles (10 × 5 mm, height × base) after sequential sonication-assisted cleaning in acetone, methanol, and methanol/water (50/50 v/v, 15 min each). As reported previously in (34), for DPS-MS analysis, a 10 μl sample solution was dropped onto the paper triangle that was placed on top of a Kimwipe to facilitate the absorption by capillarity. Desalting was achieved by loading 10 μl of acetonitrile/H_2O solution (90/10 v/v) onto the paper placed on top of another Kimwipe to wick the eluent containing salts and other chemicals. The paper triangle was then held in front of the MS inlet (8 mm away) using a high-voltage cable alligator clip, and 10 μl of acetonitrile/H_2O/formic acid solution (10/90/1 v/v/v) was added directly onto the paper triangle to elute the target compounds for ionization upon application of a high voltage (3.5 kV) to the wetted paper.

Data availability

The authors confirm that the data supporting the findings of this study are available within the article [and/or] its supplementary materials. Share upon Request.

Supporting information—This article contains Supporting information (59, 60).

Author contributions—M. B., H. C., and A. F. methodology; M. B., Q. W., T. J., A. V., T. H., M. O., and L. T. investigation; M. B., H. C., M. O., L. T., and A. F. formal analysis; M. B. and A. F. writing–original draft; M. B., Q. W., T. J., A. V., T. H., M. O., L. T., H. C., and A. F. writing–review and editing.

Funding and additional information—This work was supported by an USDA-NIFA award (Accession #1019179) to A. F. and H. C. and an NSF award (CHE-2203284) to H. C. and M. H.

Conflict of interest—The authors declare that they have no conflicts of interest with the contents of this article.

Abbreviations—The abbreviations used are: AG, arabinogalactan; AGP, arabinogalactan protein; CAb, capture antibody; cDNA, complementary DNA; DPS-MS, desalting paper spray-mass spectrometry; FUT, fucosyltransferase; GT, glycosyltransferase; IgG, immunoglobulin G; *i*-GT-ray, *in vitro* GT-array; IVTT, *in vitro* transcription/translation; MS, mass spectrometry; NAPPA, nucleic acid programmable protein array; NDP, nucleotide diphosphate; PBS, phosphate buffered saline; PPI, protein-protein interaction; RG, rhamnogalacturonan.

References

1. Lairson, L. L., Henrissat, B., Davies, G. J., and Withers, S. G. (2008) Glycosyltransferases: structures, functions, and mechanisms. *Annu. Rev. Biochem.* **77**, 521–555
2. Amos, R. A., and Mohnen, D. (2019) Critical review of plant cell wall matrix polysaccharide glycosyltransferase activities verified by heterologous protein expression. *Front. Plant Sci.* **10**, 915
3. Welner, D. H., Shin, D., Tomaleri, G. P., DeGiovanni, A. M., Tsai, A. Y.-L., Tran, H. M., *et al.* (2017) Plant cell wall glycosyltransferases: high-throughput recombinant expression screening and general requirements for these challenging enzymes. *PLoS One* **12**, e0177591
4. Bacic, A., Harris, P., and Stone, B. (1988) Structure and function of plant cell walls. In: Priess, J., ed. *The Biochemistry of Plants*, Academic Press, New York/London/San Francisco: 297–371
5. Carpita, N. C., and Gibeaut, D. M. (1993) Structural models of primary cell walls in flowering plants: consistency of molecular structure with the physical properties of the walls during growth. *Plant J.* **3**, 1–30
6. Fry, S. C. (2011) Cell wall polysaccharides and covalent crosslinking. *Annu. Plant Rev.* **41**, 1–42
7. Reiter, W.-D., Chapple, C. C. S., and Somerville, C. R. (1993) Altered growth and cell walls in a fucose-deficient mutant of *Arabidopsis*. *Science* **261**, 1032–1035
8. Ryden, P., Sugimoto-Shirasu, K., Smith, A. C., Findlay, K., Reiter, W.-D., and McCann, M. C. (2003) Tensile properties of Arabidopsis cell walls depend on both a xyloglucan cross-linked microfibrillar network and rhamnogalacturonan II-borate complexes. *Plant Physiol.* **132**, 1033–1040
9. O'Neill, M. A., Eberhard, S., Albersheim, P., and Darvill, A. G. (2001) Requirement of borate cross-linking of cell wall rhamnogalacturonan II for Arabidopsis growth. *Science* **294**, 846–849
10. Panter, P. E., Kent, O., Dale, M., Smith, A. J., Skipsey, M., Thorlby, G., *et al.* (2019) MUR1-mediated cell-wall fucosylation is required for freezing tolerance in *Arabidopsis thaliana*. *New Phytol.* **224**, 1518–1531
11. Panter, P. E., Seifert, J., Dale, M., Pridgeon, A. J., Hulme, R., Ramsay, N., *et al.* (2023) Cell wall fucosylation in Arabidopsis influences control of leaf water loss and alters stomatal development and mechanical properties. *J. Exp. Bot.* **74**, 2680–2691
12. Voxeur, A., Soubigou-Taconnat, L., Legee, F., Sakai, K., Antelme, S., Durand-Tardif, M., *et al.* (2017) Altered lignification in *mur1–1* a mutant deficient in GDP-L-fucose synthesis with reduced RG-II cross linking. *PLoS One* **12**, e0184820
13. Mohnen, D. (2008) Pectin structure and biosynthesis. *Curr. Opin. Plant Biol.* **11**, 266–277
14. Waldron, K. W., and Faulds, C. B. (2007) Cell wall polysaccharides: composition and structure. *Chem. Mol. Sci. Chem. Eng.* **1**, 181–201
15. Ndeh, D., Rogowski, A., Cartmell, A., Luis, A. S., Baslé, A., Gray, J., *et al.* (2017) Complex pectin metabolism by gut bacteria reveals novel catalytic functions. *Nature* **544**, 65–70
16. Lombard, V., Golaconda Ramulu, H., Drula, E., Coutinho, P. M., and Henrissat, B. (2014) The carbohydrate-active enzymes database (CAZy) in 2013. *Nucleic Acids Res.* **42**, D490–D495
17. Wu, Y., Williams, M., Bernard, S., Driouich, A., Showalter, A. M., and Faik, A. (2010) Functional identification of two nonredundant Arabidopsis alpha(1,2)fucosyltransferases specific to arabinogalactan proteins. *J. Biol. Chem.* **285**, 13638–13645
18. Perrin, R. M., DeRocher, A. E., Bar-Peled, M., Zeng, W., Norambuena, L., Orellana, A., *et al.* (1999) Xyloglucan fucosyltransferase, an enzyme involved in plant cell wall biosynthesis. *Science* **284**, 1976–1979
19. Faik, A., Bar-Peled, M., DeRocher, A. E., Zeng, W., Perrin, R. M., Wilkerson, C., *et al.* (2000) Biochemical characterization and molecular cloning of an alpha-1,2-fucosyltransferase that catalyzes the last step of cell wall xyloglucan biosynthesis in pea. *J. Biol. Chem.* **275**, 15082–15089
20. Liu, L., Paulitz, J., and Pauly, M. (2015) The presence of fucogalactoxyloglucan and its synthesis in rice indicates conserved functional importance in plants. *Plant Physiol.* **168**, 549–560
21. Altschul, S. F., and Koonin, E. V. (1998) Iterated profile searches with PSI-BLAST–a tool for discovery in protein databases. *Trends Biochem. Sci.* **23**, 444–447
22. Eddy, S. R. (2011) Accelerated profile HMM searches. *PLoS Comput. Biol.* **7**, e1002195
23. Kelley, L. A., Mezulis, S., Yates, C. M., Wass, M. N., and Sternberg, M. J. (2015) The Phyre2 web portal for protein modeling, prediction and analysis. *Nat. Protoc.* **10**, 845–858
24. Roberts, R. J. (2011) Combrex: computational bridge to experiments. *Biochem. Soc. Trans.* **39**, 581–583

25. Sarria, R., Wagner, T. A., O'Neill, M. A., Faik, A., Wilkerson, C. G., Keegstra, K., *et al.* (2001) Characterization of a family of Arabidopsis genes related to xyloglucan Fucosyltransferase1. *Plant Physiol.* **127**, 1595–1606
26. [preprint] Wiemels, R. E., Zeng, W., Jiang, N., and Faik, A. (2019) Characterization of xyloglucan-specific fucosyltransferase activity in Golgi-enriched microsomal preparations from wheat seedlings. *bioRxiv*. https://doi.org/10.1101/803395
27. Soto, M. J., Urbanowicz, B. R., and Hahn, M. G. (2019) Plant fucosyltransferases and the emerging biological importance of fucosylated plant structures. *CRC Crit. Rev. Plant Sci.* **38**, 1–12
28. Anderson, K. S., Sibani, S., Wallstrom, G., Qiu, J., Mendoza, E. A., Raphael, J., *et al.* (2011) Protein microarray signature of autoantibody biomarkers for the early detection of breast cancer. *J. Proteome Res.* **10**, 85–96
29. Karthikeyan, K., Barker, K., Tang, Y., Kahn, P., Wiktor, P., Brunner, A., *et al.* (2016) A contra capture protein array platform for studying post-translationally modified auto-antigenomes. *Mol. Cell Proteomics* **15**, 2324–2337
30. Ramachandran, N., Hainsworth, E., Bhullar, B., Eisenstein, S., Rosen, B., Lau, A. Y., *et al.* (2004) Self-assembling protein microarrays. *Science* **305**, 86–90
31. Ramachandran, N., Raphael, J. V., Hainsworth, E., Demirkan, G., Fuentes, M. G., Rolfs, A., *et al.* (2008) Next-generation high-density self-assembling functional protein arrays. *Nat. Methods* **5**, 535–538
32. Yazakia, J., Galli, M., Kim, A. Y., Nito, K., Aleman, F., Chang, K. N., *et al.* (2016) Mapping transcription factor interactome networks using HaloTag protein arrays. *Proc. Natl. Acad. Sci. U. S. A.* **113**, 239–252
33. Javaid, T., Bhattarai, M., Venkataraghavan, A., Held, M., and Faik, A. (2024) Specific protein interactions between rice members of the GT43 and GT47 families form various central cores of putative xylan synthase complexes. *Plant J.* https://doi.org/10.1111/tpj.16640
34. Wang, Q., Bhattarai, M., Zhao, P., Alnsour, T., Held, M., Faik, A., *et al.* (2020) Fast and sensitive detection of oligosaccharides using desalting paper spray mass spectrometry (DPS-MS). *J. Am. Soc. Mass Spectrom.* **31**, 2226–2235
35. Faik, A., Desveaux, D., and Maclachlan, G. (1997) Xyloglucan galactosyl- and fucosyl-transferase activities in the cotyledons of developing nasturtium seeds. *Plant Physiol.* **114**, 716
36. Espada, A., and Rivera-Sagredo, A. (2003) Ammonium hydrogencarbonate, an excellent buffer for the analysis of basic drugs by liquid chromatography-mass spectrometry at high pH. *J. Chromatogr. A.* **987**, 211–220
37. Wilchek, M., and Bayer, E. A. (1990) Introduction to avidin-biotin technology. *Methods Enzymol.* **184**, 5–13
38. Chiu, K.-Y., Wang, Q., Gunawardena, H. P., Held, M., Faik, A., and Chen, H. (2021) Desalting paper spay mass spectrometry (DPS-MS) for rapid detection of glycans and glycoconjugates. *Int. J. Mass Spec.* **469**, 116688
39. Hassan, M. T., Chen, X., Fnu, P. I. J., Francis, J., Osonga, F. J., Sadik, O. A., *et al.* (2024) Rapid detection of per- and polyfluoroalkyl substances (PFAS) using paper spray-based mass spectrometry. *J. Hazard. Mater.* **465**, 133366
40. Reuhs, B. L., Glenn, J., Stephens, S. B., Kim, J. S., Christie, D. B., Glushka, J. C., *et al.* (2004) L-Galactose replaces L-fucose in the pectic polysaccharide rhamnogalacturonan II synthesized by the L-fucose-deficient *mur1* Arabidopsis mutant. *Planta* **219**, 147–157
41. Bonin, C. P., Freshour, G., Hahn, M. G., Vanzin, G. F., and Reiter, W. D. (2003) The GMD1 and GMD2 genes of Arabidopsis encode isoforms of GDP-D-mannose 4,6-dehydratase with cell type-specific expression patterns. *Plant Physiol.* **132**, 883–892
42. Pabst, M., Fischl, R. M., Brecker, L., Morelle, W., Fauland, A., Köfeler, H., *et al.* (2013) Rhamnogalacturonan II structure shows variation in the side chains monosaccharide composition and methylation status within and across different plant species. *Plant J.* **76**, 61–72
43. Atmodjo, M., Hao, Z., and Mohnen, D. (2013) Evolving views of pectin biosynthesis. *Annu. Rev. Plant Biol.* **64**, 747–779
44. Tan, L., Qiu, F., Lamport, D. T., and Kieliszewski, M. J. (2004) Structure of a hydroxyproline (Hyp)-Arabinogalactan polysaccharide from repetitive Ala-Hyp expressed in transgenic Nicotiana tabacum. *J. Biol. Chem.* **279**, 13156–13165
45. Thomas, J. R., Darvill, A. G., and Albersheim, P. (1989) Isolation and structural characterization of the pectic polysaccharide rhamnogalacturonan II from walls of suspension-cultured rice cells. *Carbohydr. Res.* **185**, 261–277
46. Ohashi, H., Ohashi, T., Misaki, R., and Fujiyama, K. (2019) *Arabidopsis thaliana* α1,2-l-fucosyltransferase catalyzes the transfer of l-galactose to xyloglucan oligosaccharides. *FEBS Lett.* **593**, 187–194
47. Liang, Y., Basu, D., Pattathil, S., Xu, W.-L., Venetos, A., Martin, S. L., *et al.* (2013) Biochemical and physiological characterization of *fut4* and *fut6* mutants defective in arabinogalactan-protein fucosylation in Arabidopsis. *J. Exp. Bot.* **64**, 5537–5551
48. Faik, A., and Held, M. (2019) Review: plant cell wall biochemical omics: the high-throughput biochemistry for polysaccharide biosynthesis. *Plant Sci.* **286**, 49–56
49. Seifert, G. J. (2004) Nucleotide sugar interconversions and cell wall biosynthesis: how to bring the inside to the outside. *Curr. Opin. Plant Biol.* **7**, 277–284
50. Peng, J.-S., Zhang, B.-C., Chen, H., Wang, M.-Q., Wanf, Y.-T., Li, H.-M., *et al.* (2021) Galactosylation of rhamnogalacturonan-II for cell wall pectin biosynthesis is critical for root apoplastic iron reallocation in *Arabidopsis*. *Mol. Plant* **14**, 1640–1651
51. Peña, M. J., Kong, Y., York, W. S., and O'Neill, M. A. (2012) A galacturonic acid-containing xyloglucan is involved in *Arabidopsis* root hair tip growth. *Plant Cell* **24**, 4511–4524
52. Ruprecht, C., Bartetzko, M. P., Senf, D., Lakhina, A., Smith, P. J., Soto, M. J., *et al.* (2020) Glycan array-based assay for the identification and characterization of plant glycosyltransferases. *Angew. Chem. Int. Ed. Engl.* **59**, 12493–12498
53. Egelund, J., Petersen, B. L., Motawia, M. S., Damager, I., Faik, A., Olsen, C. E., *et al.* (2006) Arabidopsis thaliana RGXT1 and RGXT2 encode Golgi-localized (1,3)-alpha-D-xylosyltransferases involved in the synthesis of pectic rhamnogalacturonan-II. *Plant Cell* **18**, 2593–2607
54. O'Neill, M. A., Ishii, T., Albersheim, P., and Darvill, A. G. (2004) Rhamnogalacturonan II: structure and function of a borate cross-linked cell wall pectic polysaccharide. *Annu. Rev. Plant Biol.* **55**, 109–139
55. Soto, M. J., Prabhakar, P. K., Wang, H. T., Backe, J., Chapla, D., Bartetzko, M., *et al.* (2021) AtFUT4 and AtFUT6 are arabinofuranose-specific fucosyltransferases. *Front. Plant Sci.* **12**, 132
56. Ishikawa, D., and Taki, T. (2000) Thin-layer chromatography blotting using polyvinylidenedifluoride membrane (Far-Eastern Blotting) and its applications. *Methods Enzymol.* **312**, 145–157
57. Rennie, E. A., Hansen, S. F., Baidoo, E. E. K., Hadi, M. Z., Keasling, J. D., and Scheller, H. V. (2012) Three members of the Arabidopsis glycosyltransferase family 8 are xylan glucuronosyltransferases. *Plant Physiol.* **159**, 1408–1417
58. Barnes, W. J., Koj, S., Black, I. M., Archer-Hartmann, S. A., Azadi, P., Urbanowicz, B. R., *et al.* (2021) Protocols for isolating and characterizing polysaccharides from plant cell walls: a case study using rhamnogalacturonan-II. *Biotechnol. Biofuels* **14**, 142
59. Desveaux, D., Faik, A., and Maclachlan, G. (1998) Fucosyltransferase and the biosynthesis of storage and structural xyloglucan in developing nasturtium fruits. *Plant Physiol.* **118**, 885–894
60. Faik, A., Price, N. J., Raikhel, N. V., and Keegstra, K. (2002) An Arabidopsis gene encoding an alpha-xylosyltransferase involved in xyloglucan biosynthesis. *Proc. Natl. Acad. Sci. U. S. A.* **99**, 7797–7802
61. Neelamegham, S., Aoki-Kinoshita, K., Bolton, E., Frank, M., Lisacek, F., Lütteke, T., *et al.* (2019) Updates to the symbol nomenclature for glycans guidelines. *Glycobiology* **29**, 620–624